3-D ray-tracing in anisotropic media

Jean Luc Guiziou

ABSTRACT

The issue of adapting a fast 3-D seismic ray-tracing algorithm to anisotropic media is addressed. Two approaches are considered. A method restricted to orthotropic anisotropy leads to exact calculations of traveltimes. A second algorithm, based on linearization techniques, enables to approximate the traveltimes in the case of an inhomogeneous generally anisotropic medium, under the assumption of weak anisotropy. The two methods are discussed in terms of their potential application to reflection seismology.

INTRODUCTION

An increasing effort over the recent years has been devoted to the study of wave propagation anisotropy and to the impact of this phenomenon on seismic reflection data. Dellinger and Muir (1985) clearly explained why the conventional processing techniques, based on the assumption of isotropy, seem to work perfectly even in the presence of elliptic axisymmetric anisotropy. However, the inclusion of an anisotropic model in the data processing algorithms can be required in order to obtain an accurate image of the subsurface, for example in areas where azimuthal anisotropy is observed. Moreover, the search for oil is now evolving from structural fields to stratigraphic fields which are more difficult to uncover and for which the study of anisotropy might become a key tool. Winterstein (1986) conducted careful studies of seismic data recorded in sedimentary environment and showed that anisotropy effects were indeed indicators of lithology. Anisotropy is by essence a three dimensional phenomenon and its contribution to the interpretation of seismic data will best be exploited through the use of 3-D processing techniques. However, many of these techniques will be computationally intensive; therefore numerically less involved methods, such as the ray method, might be helpful. Babich (1961) and Červený (1972) first applied the ray method to inhomogeneous anisotropic media. Numerical implementations of these algorithms can be found in Červený et al.

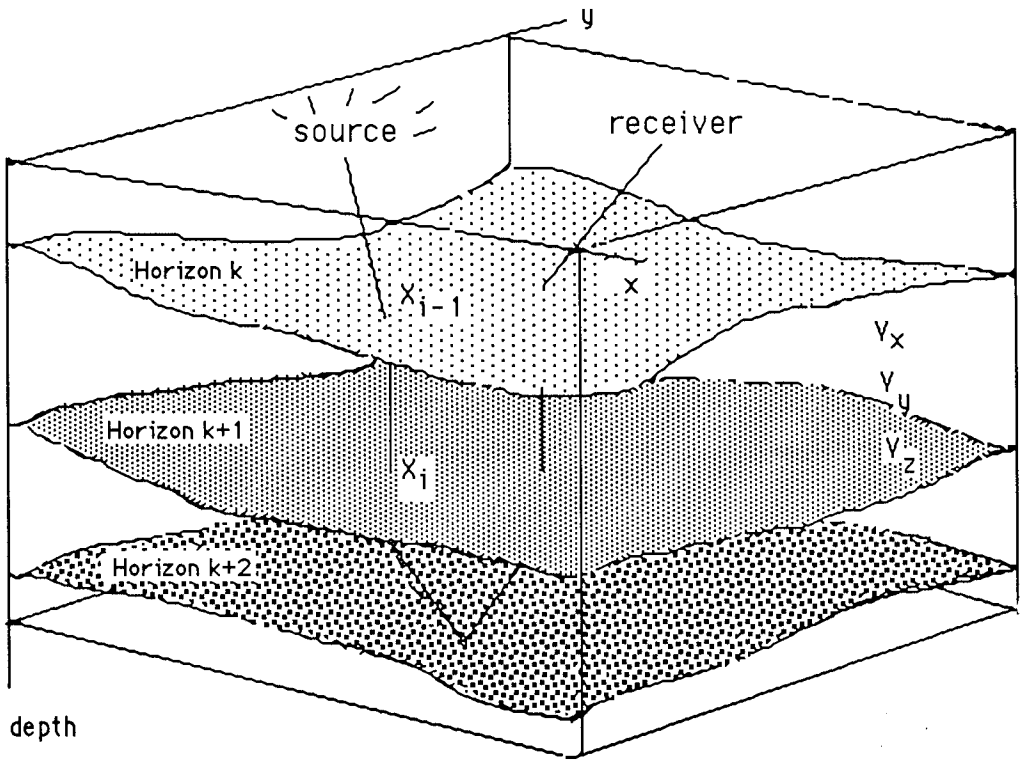

FIG. 1. A review of the ray-tracing geometry.

(1977). More recent algorithms have been developed in order to increase the efficiency of computation of synthetic seismograms, for example by using the paraxial ray approximation (Gajewski and Pšenčik, 1987).

In this paper I propose two possible approaches to include anisotropy effects in the fast 3-D ray-tracing algorithm that I presented in the last SEP report (Guiziou, SEP–56). This ray-tracing algorithm is essentially aimed at solving kinematic inverse problems for which the computation of the amplitudes is not needed. Therefore, since the computation efficiency is a major concern, a specialized algorithm devoted to traveltime calculations is preferred. Both methods to include anisotropy are easily inserted in the isotropic algorithm. The first one is restricted to an orthotropic anisotropic model but requires no additional cost with respect to the isotropic case. The second method is a little more involved but enables to consider inhomogeneous generally anisotropic media. The strengths and limitations of these two approaches are then discussed, along with their potential applications to the processing of seismic reflection data.

MODELING HOMOGENEOUS ORTHOTROPIC ANISOTROPY

In the last SEP report (Guiziou, SEP–56) I described a 3-D ray-tracing algorithm defined as the solution to a boundary value problem, using a bending method. Figure 1 depicts the geometry of the method.

The ray joining the shot and receiver after reflection on a given interface is computed so as to meet Fermat's principle. We assume that we know the signature of the ray (i.e. the succession of layers crossed) and that we can write an analytic expression for the traveltime between two points in a given layer. The raypath is then the solution to an optimization problem applied to the position of the intersection points between the ray and each interface. If the geological layers are assumed to be homogeneous and isotropic, the overall traveltime from the shot to the receiver is simply defined as:

$$t = \sum_{i=1}^{N+1} t_i = \sum_{i=1}^{N+1} \frac{D_i}{V_i} \tag{1}$$

where $(N+1)$ is the number of ray segments, D_i is is the length of the i-th segment and V_i is a constant velocity in the portion of the layer crossed by this segment.

Equation (1) can be easily modified in order to account for a certain degree of anisotropy in one or all of the geological layers. If instead of considering a unique velocity per layer we allow for three independent velocities V_x, V_y and V_z along directions parallel to the coordinate axis, we are defining an anisotropy with orthotropic symmetry. The analytic expression of the traveltime between two points $\mathbf{x}_{i-1}$ and $\mathbf{x}_i$ of a given layer remains extremely simple, namely:

$$t_i = \left[\left(\frac{x_i - x_{i-1}}{V_x^{\,i}} \right)^2 + \left(\frac{y_i - y_{i-1}}{V_y^{\,i}} \right)^2 + \left(\frac{z_i - z_{i-1}}{V_z^{\,i}} \right)^2 \right]^{1/2} . \tag{2}$$

Starting from any initial ray joining the shot and geophone, the closest ray that leads to a stationary Fermat's functional is iteratively determined by perturbing the x and y positions of the N intersection points between the ray and the interfaces. Each iteration requires to solve the following set of $2N$ equations in $2N$ unknowns:

$$\begin{cases} \phi_{2i-1} &= \frac{\partial t_i}{\partial x_i} + \frac{\partial t_{i+1}}{\partial x_i} = 0 \\ \phi_{2i} &= \frac{\partial t_i}{\partial y_i} + \frac{\partial t_{i+1}}{\partial y_i} = 0 \, ; \end{cases}$$

which can be expanded to:

$$\begin{cases} \phi_{2i-1} &= \frac{1}{t_i} \left[\frac{\Delta x_i}{\left(V_x^{\,i}\right)^2} + \frac{\Delta z_i}{\left(V_z^{\,i}\right)^2} \cdot \frac{\partial z_i}{\partial x_i} \right] - \frac{1}{t_{i+1}} \left[\frac{\Delta x_{i+1}}{\left(V_x^{\,i+1}\right)^2} + \frac{\Delta z_{i+1}}{\left(V_z^{\,i+1}\right)^2} \cdot \frac{\partial z_i}{\partial x_i} \right] = 0 \\ \phi_{2i} &= \frac{1}{t_i} \left[\frac{\Delta y_i}{\left(V_y^{\,i}\right)^2} + \frac{\Delta z_i}{\left(V_z^{\,i}\right)^2} \cdot \frac{\partial z_i}{\partial y_i} \right] - \frac{1}{t_{i+1}} \left[\frac{\Delta y_{i+1}}{\left(V_y^{\,i+1}\right)^2} + \frac{\Delta z_{i+1}}{\left(V_z^{\,i+1}\right)^2} \cdot \frac{\partial z_i}{\partial y_i} \right] = 0 \, . \end{cases}$$

A look at the algorithm described in the last report clearly shows that the inclusion of the orthotropic anisotropy requires no additional cost with respect to the isotropic assumption.

The expression for the traveltime given by equation (2) assumes that the axis of symmetry of the ellipse coincide with the cartesian axis (x, y, z) of the ray-tracing geometry. This is not too much of a constraint since the most common type of anisotropy observed in mildly deformed sedimentary basins is transverse isotropy with vertical axis of symmetry. The major source of stress in those basins is gravity; this results in a vertical principal axis for the stress. In any case, this restriction can be easily removed by assigning a local referential (x_1, x_2, x_3) to each anisotropic layer. Each ray segment simply needs to be transformed into the local referential to evaluate the traveltime in the concerned layer affected by an arbitrary orthotropic anisotropy.

MODELING INHOMOGENEOUS ARBITRARY ANISOTROPY

In the preceding section we have seen a simple way to consider a model for anisotropy in the calculations of both the raypaths and the traveltimes. However, if we keep in mind that the fast ray-tracing algorithms discussed in this paper are designed to solve inverse kinematic problems, we can allow some relaxation in the determination of the raypath and concentrate on the computation of the traveltime. This allows us to consider an alternative approach to include anisotropy in the processing scheme. This method, based on a linearization technique, was first proposed by Červený (1981) and discussed by Červený and Jech (1982). An over-simple illustration of the idea is depicted in Figure 2.

Červený and Jech demonstrated that it was possible to derive the traveltime between two points $\mathbf{x}_{i-1}$ and $\mathbf{x}_i$ in a generally inhomogeneous anisotropic medium by integrating small perturbations of the anisotropy along the path of the ray computed in a reference medium. The main restriction for the adequacy of the method is a limited difference in elastic parameters between the reference medium and the actual one. If t_i denotes the traveltime between the points $\mathbf{x}_{i-1}$ and $\mathbf{x}_i$, we have:

$$t_i(\mathbf{x}_{i-1}, \mathbf{x}_i) = t_i^0(\mathbf{x}_{i-1}, \mathbf{x}_i) + t_i^1(\mathbf{x}_{i-1}, \mathbf{x}_i),$$

where t_i^0 is the traveltime in the reference medium and t_i^1 is the perturbation of this traveltime due to the effect of anisotropy. For our purposes we will use the algorithm described in the preceding section to compute the unperturbed traveltime and we will supplement it by the determination of the perturbation t^1. This linearization technique works directly with the 21 elastic parameters c_{ijkl} and with the density ρ of the medium; hence it makes no assumption on the system of anisotropic symmetry.

In the simple case where the reference medium is isotropic, Červený and Jech (1982) have derived analytic expressions for the evaluation of the traveltime perturbation t^1. If the wave under consideration is a P wave, then t^1 is expressed

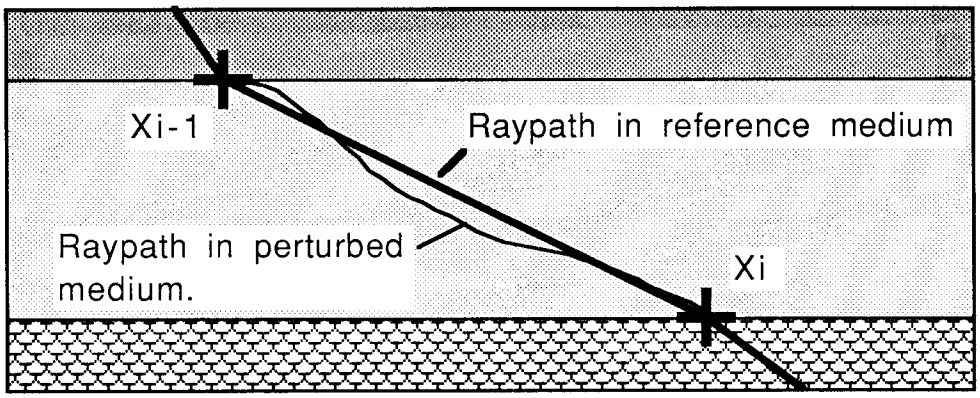

FIG. 2. Given the raypath connecting two points in some reference medium, the traveltime between these two points in a slightly different medium, in terms of anisotropy, can be estimated by integrating the perturbation in elastic parameters along the reference raypath. This linearization technique does not estimate the actual raypath in the perturbed medium.

as:

$$t^1(\mathbf{x}_{i-1},\mathbf{x}_i) = -1/2 \int_{L^0} V_p^2(\tau).p_i(\tau).p_j(\tau).p_k(\tau).p_l(\tau).a^1_{ijkl}(\tau).d\tau \ , \qquad (3)$$

where:
L^0 is the raypath in the reference medium between $\mathbf{x}_{i-1}$ and $\mathbf{x}_i$,
$d\tau$ is an elementary time step along L^0,
$V_p(\tau)$ is the P wave velocity in the reference medium, at position $\mathbf{x}(\tau)$,
$p_1(\tau), p_2(\tau), p_3(\tau)$ are the components of the slowness vector along the raypath in the reference medium, at position $\mathbf{x}(\tau)$, and
$a^1_{ijkl}(\tau)$ is the residual elastic tensor between the reference medium and the actual medium, at location $\mathbf{x}(\tau)$.

As we can see from Equation (3), the attributes of the ray in the unperturbed medium are treated as weighting factors applied to the variations in elastic parameters. The presence of the dummy variable τ in all the terms of the integrand allows for inhomogeneities both in the reference and the actual media.

Concerning the propagation of S waves, the choice of an isotropic reference medium is somewhat ambiguous because the S_H and S_V waves coincide and the determination of a time perturbation for each type of wave cannot be achieved. We only get the average time correction to be applied to the shear waves (Červený and Jech, 1982). A general expression for the computation of the traveltime perturbation for P, S_V and S_H waves in the case where the reference medium is anisotropic and

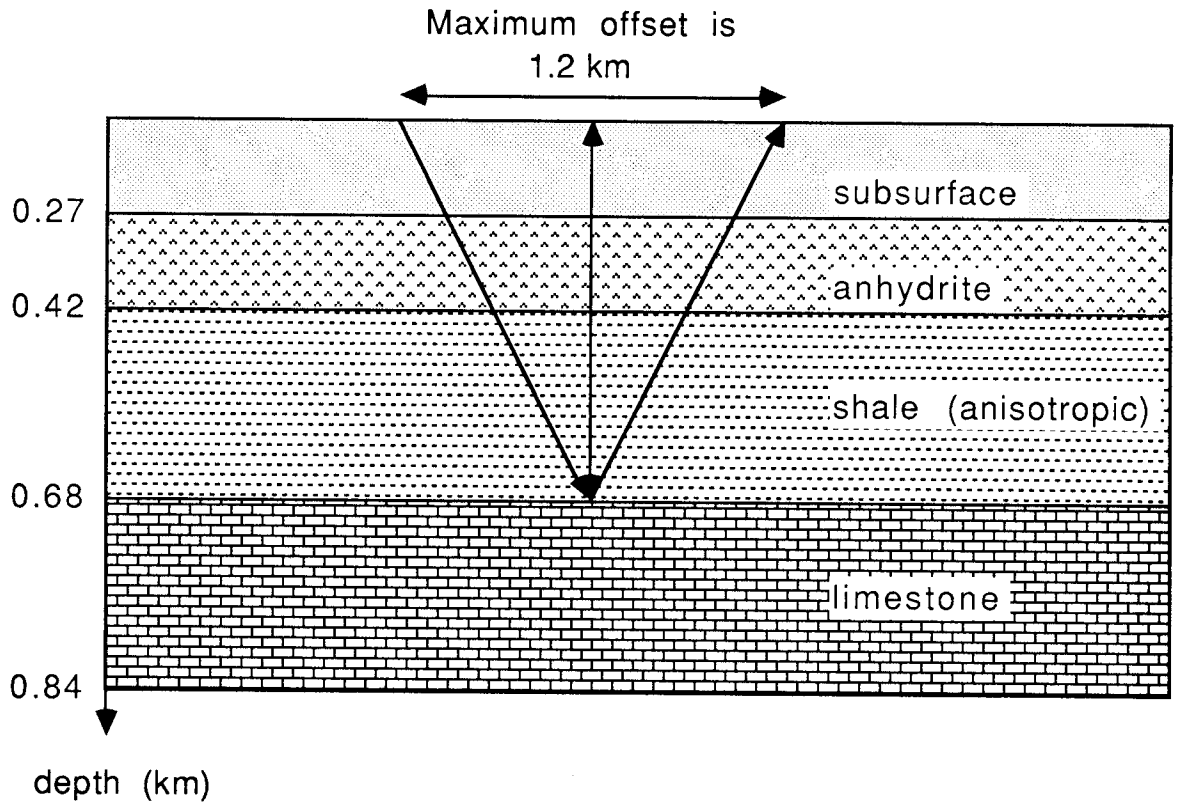

FIG. 3. This stack of layers is illuminated by a CMP gather with a maximum offset of 1.2 km in order to study how the anisotropic layer of shale affects the traveltime curve.

the anisotropy has an orthotropic symmetry can be derived from the equations proposed by Červený and Jech (1982).

APPLICATION TO REFLECTION SEISMOLOGY

A better fit to the data

Reflection seismology surveys have long been poorly adapted to the study of anisotropy because they could handle almost exclusively compressionnal waves propagating along quasi-vertical directions. Long-cable surveys (96 channels) and three-component recording have now become more routine and provide data which can show evidences of anisotropy effects. The ray-tracing method described in section one has been applied to the calculation of traveltimes for a CMP gather illuminating a realistic subsurface in order to measure the influence of anisotropy. Figure 3 depicts the geological model considered. The restriction to horizontal interfaces between the layers will prevent any coupling between structural effects and effects

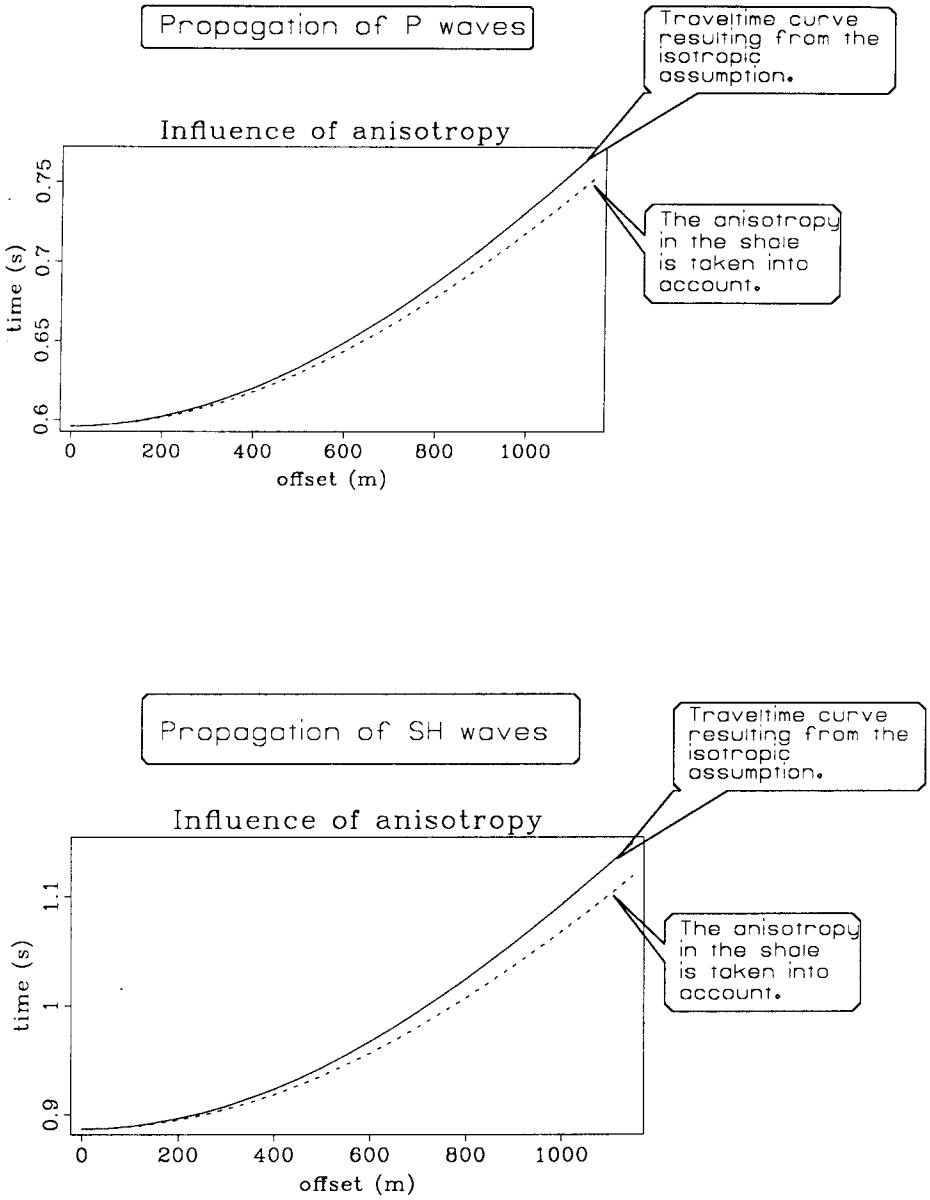

FIG. 4. The traveltime curves corresponding to the CMP gather presented on Figure 3 have been computed for the P and SH waves. The inclusion of the anisotropic character of the shale in the ray-tracing algorithm yields a noticeable perturbation of the traveltimes.

due to the anisotropy. The overall transverse isotropic nature of the subsurface comes from a layer of shale which has intrinsic anisotropic properties. The CMP gather contains 48 offsets, 25 meters apart from each other. This geometry leads to a maximum offset of 1.2 km and to wave propagation angles up to 40 degrees with respect to the vertical. The traveltimes corresponding to the propagation of the P and S_H waves have been computed under the assumption of transverse isotropy. For the P-wave, the horizontal and vertical velocities in the shale are respectively 2990 m/s and 2650 m/s. For the S_H-wave these velocities are V_{SH}^h =1750 m/s and V_{SH}^v =1450 m/s. In order to measure the influence of anisotropy effects due to the layer of shale, the same CMP gather has been computed in the case where the shale is treated as isotropic, with a velocity equal to the true vertical velocity for each type of wave. The comparative traveltime curves are displayed on Figure 4. The effect of the anisotropy on the P-wave can be noticed on records with an offset greater than 0.6 km. For this particular offset the difference in traveltime between the isotropic and anisotropic assumptions reaches 5 milliseconds, which I consider as the minimal significant variation for a traveltime inversion application. The discrepancy between the two curves increases up to 16 milliseconds, which is the value obtained for the maximum offset of 1.2 km. In terms of propagation angles, the anisotropy due to the layer of shale can be detected by recording P-waves travelling at an angle greater than 20 degrees with respect to the vertical.
The S_H wave is more sensitive than the P wave to the presence of the layer of shale. The traveltime perturbation becomes noticeable when the offset reaches 0.4 km, which corresponds to an angle of propagation of 15 degrees with respect to the vertical. The maximum offset shows a 30 milliseconds difference in traveltime between the isotropic case and the anisotropic one.
This simple synthetic example suggests that the inclusion of anisotropy in data processing algorithms can help in obtaining a better fit to the data, particularly when the depths of the horizons are constrained by well-log measurements. Also, for a traveltime inversion application, the ability to model and invert anisotropic properties might help in detecting lateral variations of the lithology.

Accuracy of the traveltimes

The ray-tracing algorithm specialized to the case of anisotropy with orthotropic symmetry leads to exact calculations of the traveltimes, under the assumption of elliptic impulse responses for the P and S waves. On the other hand, the algorithm based on the linearization technique computes only approximate traveltimes. Before a further discussion on the adequacy of the methods for processing seismic data, we need to compare the two approaches and study the consistency of their results.
The linearization technique requires a small variation of the anisotropy between the reference medium and the actual one. This is not a severe limitation because most realistic geological models show only weak anisotropic properties and an isotropic reference medium is often adequate. In this section we discuss a comparison of the two algorithms in the case of an extremely simple model. We consider a unique CMP

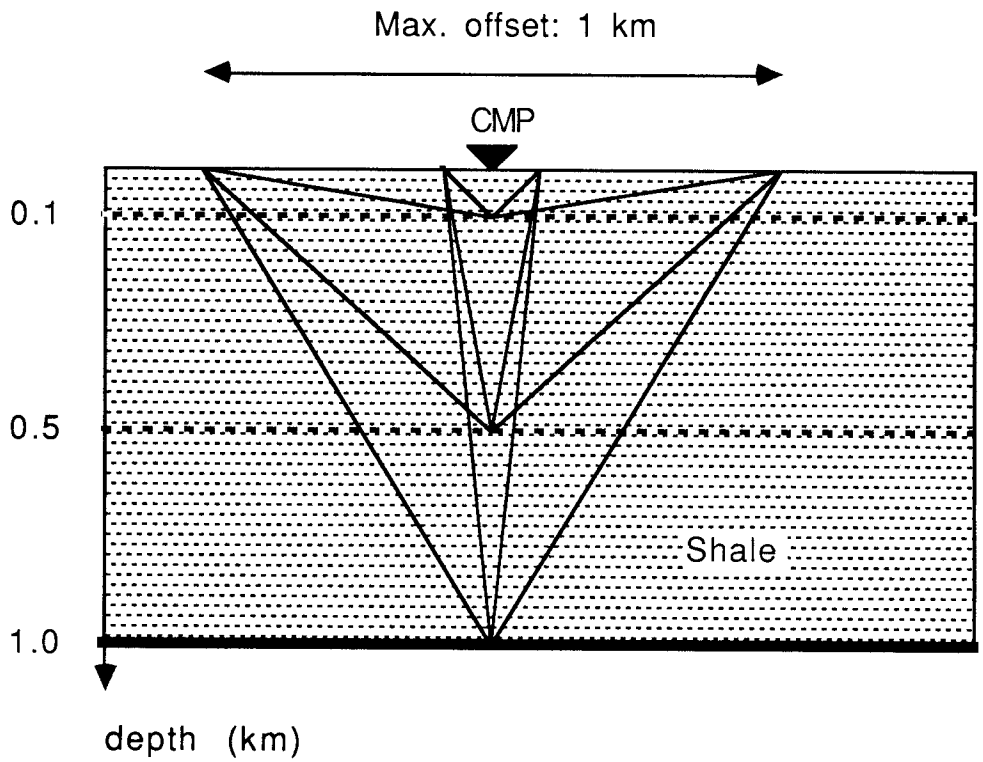

FIG. 5. Traveltimes for a CMP gather recorded over a unique layer of shale are computed. The experiment is repeated for three different depths of the reflector, in order to study a broader range of wave propagation angles.

gather recorded over a layer of shale characterized by an axisymmetric anisotropy. The geometry of this test case is illustrated in Figure 5. The plots presented on figures 6,7 and 8 comment upon the influence of the reference medium on the accuracy of the *P*-wave traveltimes computed by linearization. We also let the depth of the reflector vary, in order to consider a variety of wave propagation angles ranging from zero to about eighty degrees, with respect to the vertical. A look at the different curves shows clearly that the linearization technique is noticeably influenced by the reference medium and the propagation angle of the waves. In our case limited to a transverse isotropic medium, the choice of an isotropic reference velocity equal to the average of the true horizontal and vertical velocities leads to reasonably accurate traveltime computations.

Evaluation of the methods

Since the two traveltime computation algorithms described in this paper differ by a number of important characteristics (description of the medium, accuracy of the traveltimes, etc) the choice of one of the two methods will depend strongly on the seismic application of interest and on the geological model to be considered. The first method, referred to as the "orthotropic method", enables to consider a

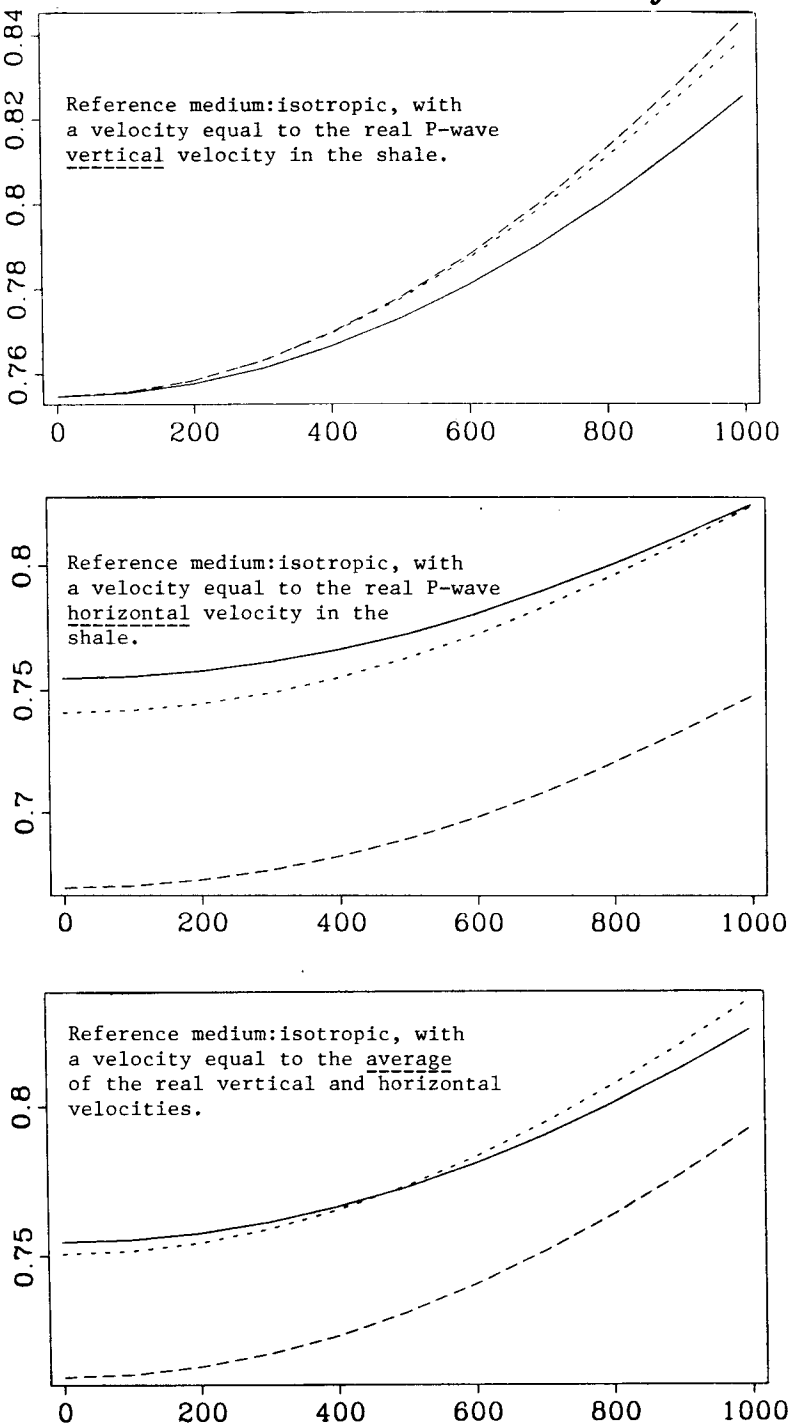

FIG. 6. Traveltime curves for the CMP gather described on Figure 5. The reflector is 1 km deep, which results in a maximum wave propagation angle of 26 degrees with respect to the vertical. Each plot corresponds to a different reference medium for the linearization technique. The solid line is the traveltime curve computed by the orthotropic algorithm. We take it here as a reference, in order to judge the accuracy of the linearization. The dashed line is the traveltime curve computed in the isotropic reference medium. The dotted curve corresponds to the traveltimes determined by linearization. This curve is expected to be as close as possible to the solid one. For this geometry, the best result is obtained by considering an average velocity for the reference medium. The isotropic material based on the real vertical velocity yields a poor result. This is an important point to notice because the vertical velocity is the one that we obtain from well-log measurements.

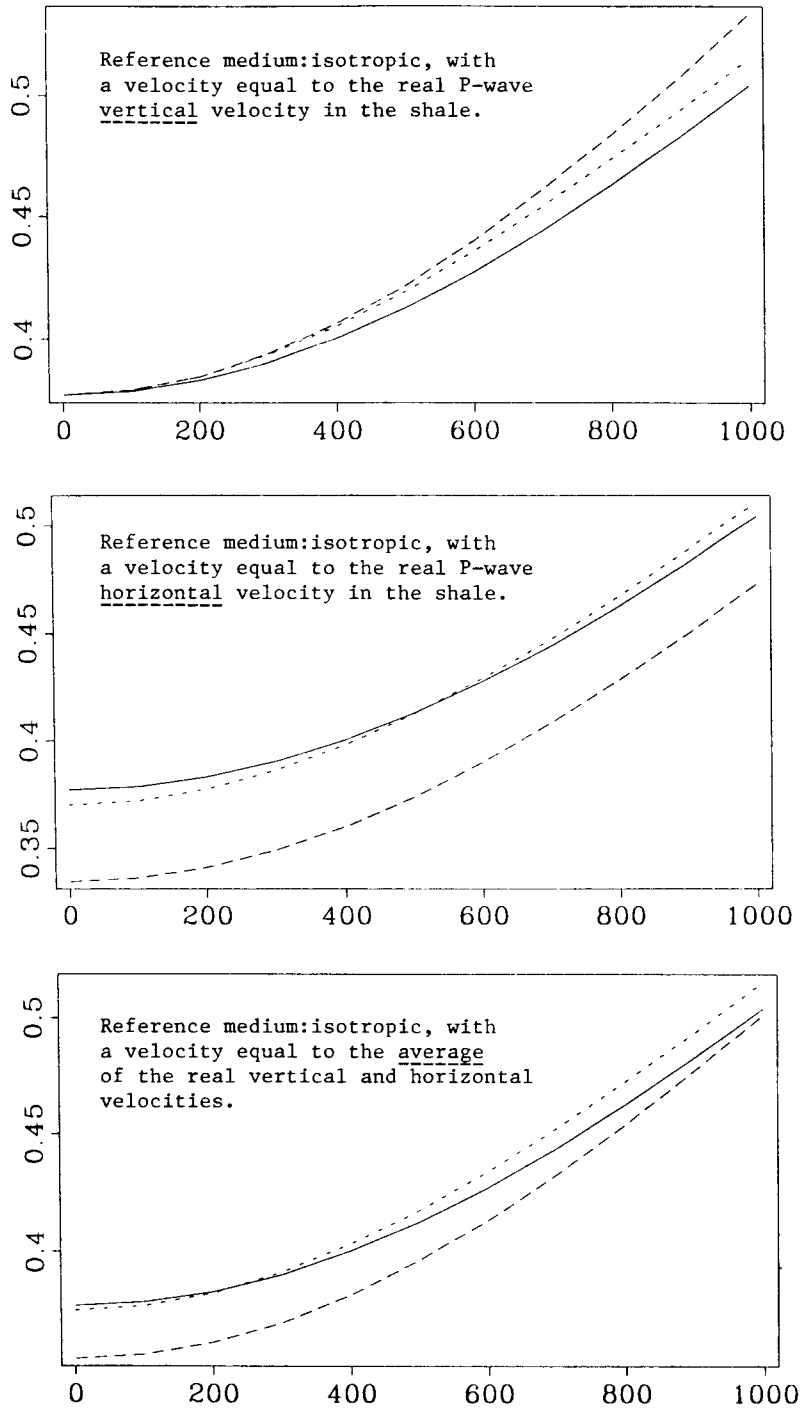

FIG. 7. If we set the depth of the reflector to 0.5 km, the propagation angles of the waves increase up to 45 degrees for the maximum offset. The three plots show the behavior of the linearization algorithm for different reference media. As in the previous figure, we can see that the isotropic medium based on the real vertical velocity does not yield a good fit to the solid line. The real horizontal velocity seems to be the most appropriate reference medium. The average velocity gives satisfying results too, especially for propagation angles inferior to 20 degrees with respect to the vertical.

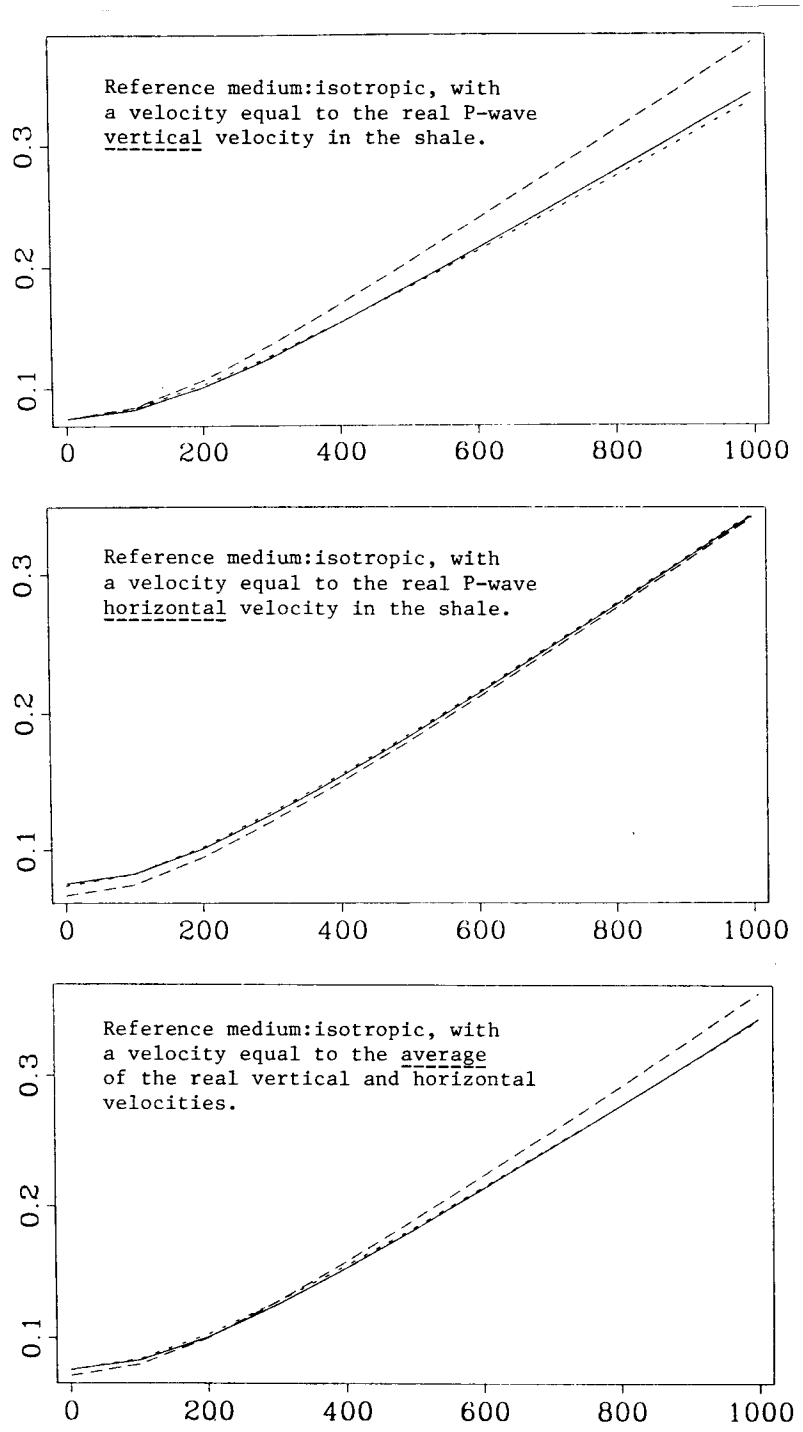

FIG. 8. The results on this figure correspond to a very shallow reflector (depth at 0.1 km). Most of the waves recorded by the CMP gather have a predominant horizontal direction of propagation. For this case the reference medium does not affect the accuracy of the linearization.

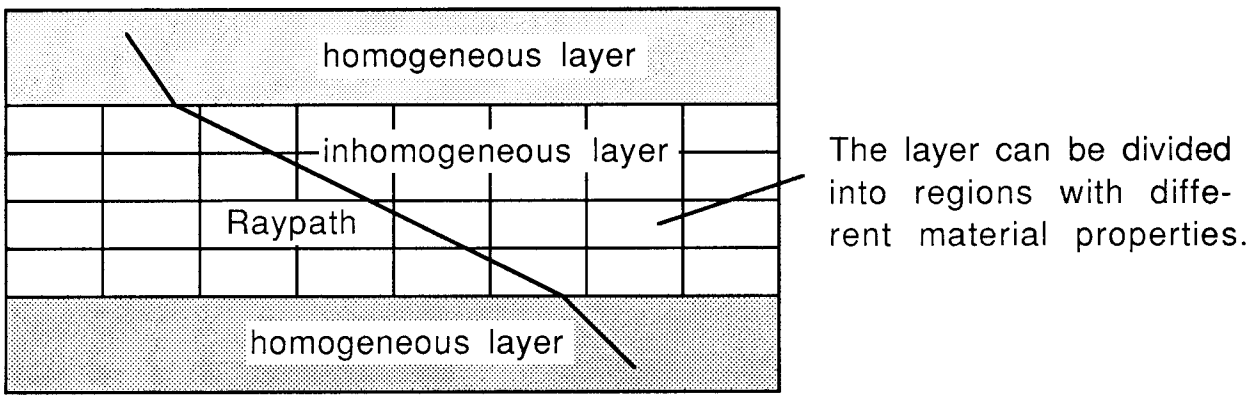

FIG. 9. The linearization formulation allows spatially variable elastic parameters. The traveltime perturbation in the inhomogeneous layer is weighted by the length of the raypath within each box.

useful model for the earth, particularly if the arbitrary orientation of the axis of symmetry of the anisotropy is implemented. The most common anisotropy symmetries observed in sedimentary basins can be accurately handled by this algorithm. Besides, for a traveltime inversion application, this model for the anisotropy can be expected to remain within the resolving power of the seismic tools. The major limitation of the orthotropic method comes from the difficulty to extend it to inhomogeneous geological layers. This can be an important issue if the study of the anisotropy is aimed at helping the geophysicist to detect lateral variations of the lithology within the earth.

The linearization method is free from any constraint on the system of symmetry of the anisotropy. This might be useful when dealing with complicated geological features for which the origin of the anisotropy is not clear. However, the 22 parameters defining a generally anisotropic medium cannot be reasonably resolved by the seismic data without external information. A traveltime inversion application based on the linearization technique will require the identification of the elastic parameters which play a significant role in the kinematics of the wave propagation. The main strength of the linearization algorithm for an application in seismic data processing is the adequacy of the formulation for inhomogeneous media. As demonstrated by Equation (3), the perturbation in elastic parameters can be a continuous function of the position on the reference raypath. In practice it will be easier to describe an inhomogeneous layer by a number of blocks within which the material properties remain constant. This approach is illustrated by Figure 9.

Dave Nichols (this SEP report) has designed a set of tools to create a grid of elastic tensors within a layer to model fairly complicated rock properties. His work can be directly applied to ray-tracing to obtain realistic geological features such as

fractured rocks, lateral variations of the lithology, etc.
I have not discussed in this paper the phenomenon of wave-type conversion. The algorithms presented here can be easily extended to handle this feature. The implementation of the type conversions will be very useful to study seismograms obtained by using a vertical source and an array of three-component geophones.

CONCLUSIONS

The inclusion of anisotropy in a fast 3-D ray-tracing algorithm can be achieved without any significant loss of performance. The algorithm restricted to orthotropic anisotropy leads to exact calculations of the traveltimes and provides a useful model for the earth. This model for the anisotropy involves a limited number of parameters which can be reasonably resolved by traveltime inversion. The algorithm based on the linearization technique enables to consider a broader range of material properties but this is achieved at the cost of some loss in the accuracy of the traveltimes. The linearization method is particularly well adapted to inhomogeneous media and can be very useful to study spatial variations of the lithology.

ACKNOWLEDGMENTS

I would like to thank Francis Muir and Dave Nichols for many fruitful discussions on anisotropy. Thanks also to Dirk Gajewski for clarifying some obscure points and for suggesting me to consider the linearization technique.
Finally, I want to express my gratitude to TOTAL CFP for supporting my stay and study at Stanford.

REFERENCES

Babich, V. M., 1961, Ray method for the computation of the intensity of wave fronts in elastic inhomogeneous anisotropic medium: Problems of the Dynamic Theory of Propagation of Seismic Waves, 5, 36-46, Leningrad University Press.

Červený, V., 1972, Seismic rays and ray intensities in inhomogeneous anisotropic media: Geophys. J. R. astr. Soc., **29**, 1-13.

Červený, V., Molotkov, I. A., Pšenčik, I., 1977, Ray method in seismology: Charles Univ. Press, Prague.

Červený, V., 1981, Direct and inverse kinematic problems for inhomogeneous anisotropic media: Contributions of the Geophysical Inst. of the Slovak Acad. Sci., Vol.13

Červený, V. and Jech, J., 1982, Linearized Solutions of Kinematic Problems of Seismic Body Waves in Inhomogeneous Slightly Anisotropic Media: J. Geophys., **51**, 96-104.

Dellinger, J. and Muir, F., 1985, Axisymmetric anisotropy I: Kinematics: SEP–**42**, 1-23.

Gajewski, D. and Pšenčik, I., 1987, Computation of high-frequency seismic wavefields in 3-D laterally inhomogeneous anisotropic media: Geophys. J. R. astr. Soc., **91**, 383-411.

Guiziou, J. L., 1987, 3-D ray-tracing: Application to tomography: SEP–**56**, 93-119.

Nichols, D., 1988, Building anisotropic models: SEP–**57**.

Winterstein, D. F., 1986, Anisotropy effects in P-wave and SH-wave stacking velocities contain information on lithology: Geophysics, **51**, 661-672.

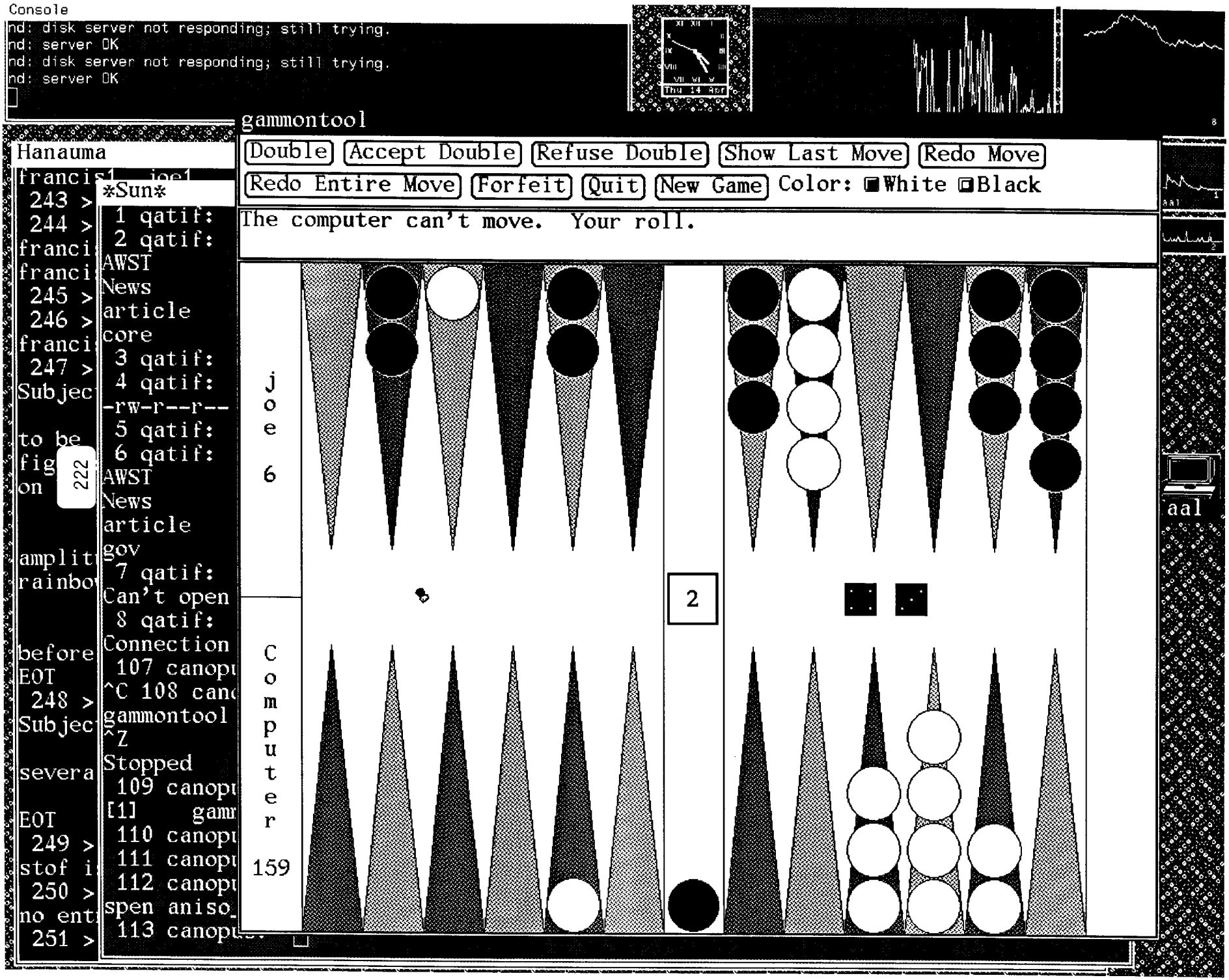

A quick game of BackGammon before turning in.